ORIGINAL ARTICLE

ETRI Journal WILEY

Millimeter-wave diffraction-loss model based on over-rooftop propagation measurements

Kyung-Won Kim (iD) | **Myung-Don Kim** | **Juyul Lee** (iD) | **Jae-Joon Park** |
Young Keun Yoon (iD) | **Young Jun Chong**

Telecommunication and Media Research Laboratory, Electronics and Telecommunications Research Institute, Daejeon, Rep. of Korea

Correspondence
Kyung-Won Kim, Telecommunication and Media Research Laboratory, Electronics and Telecommunications Research Institute, Daejeon, Rep. of Korea.
Email: kimkw@etri.re.kr

Measuring the diffraction loss for high frequencies, long distances, and large diffraction angles is difficult because of the high path loss. Securing a well-controlled environment to avoid reflected waves also makes long-range diffraction measurements challenging. Thus, the prediction of diffraction loss at millimeter-wave frequency bands relies on theoretical models, such as the knife-edge diffraction (KED) and geometrical theory of diffraction (GTD) models; however, these models produce different diffraction losses even under the same environment. Our observations revealed that the KED model underestimated the diffraction loss in a large Fresnel-Kirchhoff diffraction parameter environment. We collected power-delay profiles when millimeter waves propagated over a building rooftop at millimeter-wave frequency bands and calculated the diffraction losses from the measurements while eliminating the multipath effects. Comparisons between the measurements and the KED and GTD diffraction-loss models are shown. Based on the measurements, an approximation model is also proposed that provides a simple method for calculating the diffraction loss using geometrical parameters.

KEYWORDS
5G channel, clutter loss, diffraction loss, millimeter-wave channel, path loss

1 | INTRODUCTION

Millimeter-wave frequency bands ranging from 24 GHz to 86 GHz have received worldwide attention because of their potential use in fifth-generation (5G) international mobile telecommunication (IMT). Studies on millimeter-wave propagation characteristics are required to design and evaluate 5G systems and launch 5G services. Obstruction due to clutter frequently occurs in IMT environments; therefore, the diffraction loss is a critical propagation characteristic of IMT. For example, propagation over a building rooftop is a scenario wherein signal interference occurs between IMT and

other communication services. Figure 1 shows an example of a scenario wherein a 5G interference signal propagates over the building rooftops by diffraction. In sharing and coexistence studies between 5G and other services, the diffraction loss over a building rooftop is a critical issue when predicting signal interference levels.

The diffraction loss has been frequently used to predict wireless channels. The Walfisch path loss model was proposed by [1] for urban environments using reflection and diffraction losses over building rooftops. The Erceg path loss model was proposed by [2] for urban and suburban environments using reflection and diffraction losses around a building corner. Lu
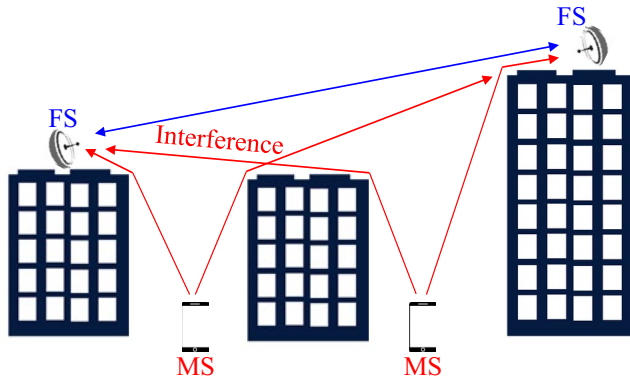
FIGURE 1 Interference scenario from 5G mobile stations (MSs) to the fixed services (FSs)

proposed a path loss model in [3] for urban street canyon environments using the geometrical theory of diffraction (GTD) [24]. Clutter-loss models based on the diffraction-loss calculation were also introduced in [4] and [5]. Chizhik proposed the path gain prediction method [4] for use when geometrical parameters of clutter are given. Recommendation ITU-R P.452 [6] introduced a clutter-loss model, and an extension of this model based on diffraction-loss calculation was proposed in [5]. 5G channel characteristics based on ray-tracing simulations were introduced in [7–9] using diffraction-loss calculations. Predicting the diffraction loss relies on theoretical models, such as the knife-edge diffraction (KED) [23] model and GTD models; however, these models produced different results up to 30 dB and 15 dB in cases of a long distance [10] or large diffraction angle [11], respectively. In [10] and [11], the KED model underestimated the diffraction losses compared to the GTD model.

Various diffraction-loss measurements were proposed in [12–20] to formulate and verify the diffraction models. Diffraction losses at frequencies from 4 GHz to 16.4 GHz and diffraction losses at 25 GHz were, respectively, proposed in [12] and [13], where an electromagnetic wave propagates over a thick screen. Diffraction losses at 25 GHz were proposed in [14], where an electromagnetic wave propagates over multiple screens. Diffraction losses around a corner at 60 GHz and 300 GHz were proposed in [15]. However, since the diffraction losses in [12–15] were measured in small chambers, they did not include the case of long-distance propagation. Outdoor diffraction measurements were performed in [16–20]. Diffraction measurements around a corner were proposed in [16–19]. Diffraction losses in [16–18] were measured at frequencies from 10 GHz to 60 GHz, but the propagation distances of their measurements were shorter than 10 m. Diffraction losses in [19] were measured at a low frequency of 1.823 GHz. Measurements in [10] and [20] revealed diffraction losses over 5 km and 1 km, respectively. However, their diffraction angles were smaller than 1.15° and 15°, respectively. Because of the high path loss, the diffraction measurements in [12–20] were limited by the short distance, low frequency, or small diffraction angle.

Based on the KED model, the diffraction loss can be calculated using the Fresnel-Kirchhoff diffraction parameter. The Fresnel-Kirchhoff diffraction parameter is a dimensionless parameter that represents the magnitude of phase difference a diffracted wave exhibits when compared to a straight path. A long distance, high frequency, and large diffraction angle are factors that make the Fresnel-Kirchhoff diffraction parameter increase. According to our observation, the KED model underestimated the diffraction loss in a large Fresnel-Kirchhoff diffraction parameter environment. 5G in an urban environment is a typical scenario of a large Fresnel-Kirchhoff diffraction parameter, where building obstacles are tall and near mobile stations. Our previous measurement results at 28 GHz were reported in [21], which introduced diffraction-loss measurements with diffraction angles from 0° to 50° and distances from 12 m to 160 m. With the same environment, we remeasured the diffraction losses at 28 GHz, 32.4 GHz, and 38 GHz. The height of the receiver (RX) was accurately adjusted to be the same height as a building rooftop edge. The measurement results were introduced in [22]. In this paper, we analyzed the relationships between the diffraction loss, distance, and frequency based on the measurements. A diffraction-loss approximation with geometrical parameters is also proposed. The remainder of the paper is organized as follows, Section 2 introduces three diffraction-loss models for comparison. Section 3 explains the channel sounder and measurement methods. In Section 4, the measurement results are provided, and the diffraction-loss approximation model is proposed. Finally, Section 5 presents the conclusions.

2 | DIFFRACTION-LOSS MODELS

2.1 | KED model

The KED model [23] is suitable when clutter is flat and thin like a knife. It is widely used even in other clutter scenarios because of the simplicity of the calculation. Based on Huygen's principle, every point that an electromagnetic wave reaches becomes a new source point of a spherical wave. Therefore, diffracted waves can have different phases owing to the different path lengths. The KED model calculates the diffraction loss using the sum of all the diffracted waves from different path lengths using the Fresnel integral. Then, the electric field generated by the total diffracted waves can be calculated using

$$F(v) = \left| \frac{1+j}{2} \int_v^\infty e^{-j\frac{\pi}{2}t^2} dt \right|, \qquad (1)$$

where the electric field induced by diffraction is denoted by $F(v)$. The Fresnel-Kirchhoff diffraction parameter is denoted by v and is given by

$$v = 2\sqrt{\frac{\Delta}{\lambda}}, \qquad (2)$$

where the wavelength is denoted by λ, and the difference the in path lengths between a direct line-of-sight path and a diffracted wave path is denoted by Δ. When clutter does not exist, v is $-\infty$ and $F(v)$ is 1. To simplify the calculation, an approximation of diffraction loss was introduced in [26], and was computed by

$$L_{\text{KED}} = 6.9 + 20\log\left(\sqrt{(v-0.1)^2 + 1} + v - 0.1\right), \qquad (3)$$

where the diffraction loss of the KED model is denoted by L_{KED}.

2.2 | GTD model

The GTD model [24] assumes that an edge point of clutter becomes a new source point of diffracted waves. With the law of conservation of energy, the power of a diffracted wave decreases with the surface area of the wave fronts. In [24], the surface area is approximated using the Gaussian curvature, which is caused by two types of point sources: the original point source and the edge point. The GTD model can then be represented as

$$E_{\text{GTD}} = E_0 \cdot \frac{D}{s_1}\sqrt{\frac{s_1}{s_2(s_1+s_2)}} \cdot e^{-jk(s_1+s_2)}, \qquad (4)$$

where the electric field of a diffracted wave is denoted by E_{GTD}. The electric field at an original source point is denoted by E_0. The travel path lengths before and after diffraction are denoted by s_1 and s_2, respectively. The wave number is denoted by k and D is a diffraction coefficient. A power loss of a diffracted wave can be derived by the GTD model and it is computed by

$$-20\log\left|\frac{\lambda}{4\pi}\cdot\frac{E_{\text{GTD}}}{E_0}\right| = 20\log\left(\frac{4\pi}{\lambda}\frac{\sqrt{s_1 s_2(s_1+s_2)}}{|D|}\right). \qquad (5)$$

The diffraction loss is defined as the attenuation by diffraction when a line-of-sight path is obstructed by clutter. The diffraction loss based on the GTD models can be computed by

$$\begin{aligned} L_{\text{GTD}} &= 20\log\left(\frac{4\pi}{\lambda}\cdot\frac{\sqrt{s_1 s_2(s_1+s_2)}}{|D|}\right) - L_{\text{FSL}}(s) \\ &= 20\log\left(\frac{\sqrt{s_1 s_2(s_1+s_2)}}{s\cdot|D|}\right), \end{aligned} \qquad (6)$$

where

$$L_{\text{FSL}}(s) = 20\log\left(\frac{4\pi s}{\lambda}\right). \qquad (7)$$

The diffraction loss of the GTD model and the free space loss are denoted by L_{GTD} and L_{FSL}, respectively. The direct 3-dimensional distance between a diffracted wave and the original source is denoted by s. The uniform theory of the diffraction (UTD) model [25] was also derived from the assumption in (4), but the diffraction coefficients in both models are calculated differently. The GTD model has singularity at a shadow boundary and the UTD model was proposed to overcome the singularity. The calculation method for the diffraction coefficient of the UTD model was introduced in [26].

2.3 | Empirical linear approximation

The empirical linear approximation was proposed by [17] based on corner diffraction measurements at 10 GHz, 20 GHz, and 26 GHz when a propagation length is fixed to 3 m. In [17], the loss at zero-degree diffraction was estimated using the KED model (about 6 dB), and the diffraction loss linearly increased with the diffraction angle. The slopes of the model were determined based on measurements using minimum mean square error estimation, which is represented as

$$L_{\text{lin}} = n \cdot \alpha + 6.03, \qquad (8)$$

where the diffraction loss, the diffraction angle, and the slope coefficient are denoted by L_{lin}, α, and n, respectively. Based on measurements around a stone pillar corner, the proposed slope coefficients were 0.75, 0.88, and 0.96 at 10 GHz, 20 GHz, and 26 GHz, respectively. In [17], it was noted that the KED model underestimates the diffraction loss when the diffraction angle is larger than 30°.

3 | MEASUREMENT METHOD

3.1 | Channel sounder

The measurement campaign was conducted using a sliding correlator channel sounder that was developed by the Electronics and Telecommunications Research Laboratory (ETRI). The bandwidth was 500 MHz, and the chip rate was 499.96 MHz. The pseudo noise code length was 4095, and the sliding factor was 12 500. The center frequencies were 28 GHz, 32.4 GHz, and 38 GHz, and the maximum transmit power was 29 dBm. The range of the automatic gain control (AGC) was 60 dB. A dynamic range of the channel sounder is about 30 dB–51 dB, depending on an AGC level.

The maximum measurable path loss is 167 dB, 169 dB, and 163 dB at 28 GHz, 32.4 GHz, and 38 GHz, respectively. The transmitter (TX) and the RX were synchronized by a rubidium oscillator, and skew between the TX and the RX can be monitored with a 1 ns resolution.

We measured the power-delay profiles and computed the path loss using the first multipath power component only to extract the diffracted wave. This component was assumed to be a diffracted path, and the other multipaths were assumed to be reflected paths. Because the delay resolution of the channel sounder was 2 ns, we could remove the multipath components that had excess travel path lengths longer than 0.6 m. The performance evaluation of the channel sounder was shown in [27]. Figure 2 shows an example of the power-delay profile measurements over a building rooftop. For reliable diffraction losses, we applied a threshold of 15 dB from the peak noise power. If the first multipath component power was lower than the threshold, the measurem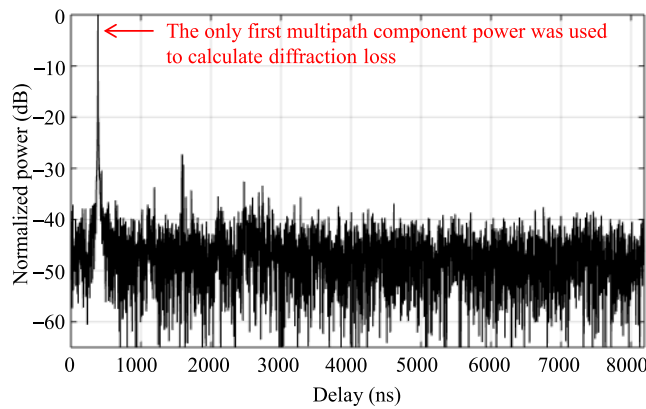ent data was discarded. When another multipath component was stronger than the first multipath component, the measurement data was also discarded because a substantial AGC attenuation caused by the strongest path can cause a power calculation error due to the analog to digital converter range.

3.2 | Measurement scenarios

We measured the diffraction losses over a building rooftop in the environment shown in Figure 3. The building is the tallest in the region, and there is no other building in front of or behind the building. We chose this building only to capture a diffracted wave and avoid reflected waves by other buildings. The height of the building was 14 m, including the guard rails, and the height of the guard rail was 1.1 m. An RX was located on the rooftop, and the height was also 14 m from the ground. A TX was located on the ground, and its height was 2 m or 4 m. Horn antennas were used for the TX and the RX. The boresights of the TX and RX were fixed at the rooftop edge. The RX antenna direction was fixed to 90°, but the TX antenna direction should be rotated depending on the location. If we use an extremely narrow beam-width antenna, a small alignment error can cause a large power calculation error. Therefore, the 30° horn antenna was used for the TX to reduce the alignment error. The 10° horn antenna was used for the RX to reduce the multipath effect as much as possible, which was the narrowest beam-width antenna in antennas available. The TX was located 8 m–110 m from the building. The RX was located 1m–40 m from the building rooftop edge. The diffraction angles corresponding to the TX locations were from 6° to 56°. Figure 4 and Table 1 show the geometrical parameters for formulation. The distance from the TX to the building is denoted by d_b. The distance from the TX to the edge of the building rooftop is denoted by d_1. The distance from the edge of the building rooftop to the RX

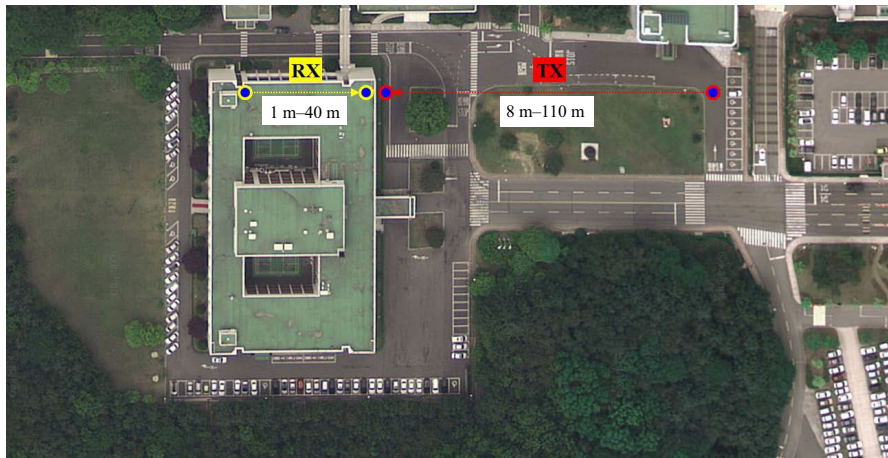**FIGURE 2** An example of the power-delay profile measurements

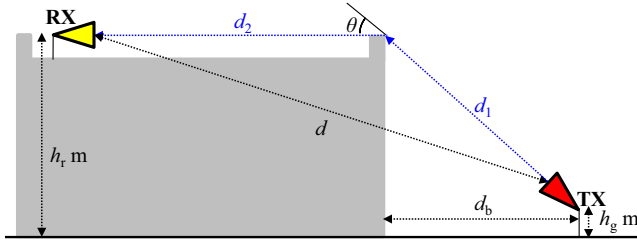**FIGURE 3** Top view of the measurement environment

FIGURE 4 Side view of the measurement environment and geometrical parameters for formulation

is denoted by d_2. The direct 3-dimensional distance from the TX to the RX is denoted by d. The diffraction angle is denoted by θ. The heights of the TX and RX are denoted by h_g and h_r, respectively.

There were three types of measurement scenarios, and the geometrical parameters are shown in Table. The scenario S1 is the main scenario to measure diffraction losses. We measured the diffraction losses at 28 GHz, 32.4 GHz, and 38 GHz, and modeled the diffraction-loss calculation based on the measurements. Scenarios S2 and S3 were used to verify the results of S1. In scenario S2, the locations of the TX and RX were interchanged to check the reciprocity of the diffraction-loss measurements. In scenario S3, the height of the TX was changed while maintaining the diffraction angles constant to determine the relationship among the diffraction loss, diffraction angle, and distance (Table 1).

4 | MEASUREMENT RESULTS AND APPROXIMATION

4.1 | Reference path loss measurement

The path loss from the first multipath power component was computed by

$$L_{PL} = P_{TX} + G_{TX} + G_{RX} + G_{sys} - (P_{RX} + A + B), \quad (9)$$

where the path loss, transmitted power, TX antenna gain, RX antenna gain, RX system gain, and the first multipath power component are denoted by L_{PL}, P_{TX}, G_{TX}, G_{RX}, G_{sys}, and P_{RX}, respectively. An attenuation by the AGC is denoted by A. An offset value of the processing gain and the system response compensation (deconvolution) gain [27] is denoted by B.

We measured the reference path loss in an environment of Figure 5. For the reference measurement, d_2 was fixed to zero, and the RX antenna was tilted to the TX antenna. The height of the RX antenna was 0.4 m from the guard rail. As shown in Figure 6, the reference path losses were approximately equal to the free space loss. The maximum difference between a reference path loss and free space loss was less than 2 dB.

4.2 | Diffraction-loss measurement

In this paper, the diffraction loss is defined as the increase in the path loss caused by building obstructions if the only power of a diffracted wave captured in the first multipath power
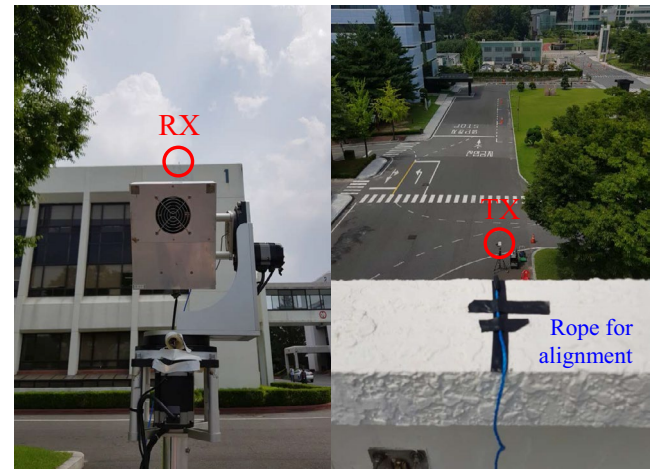

FIGURE 5 Reference path loss measurement environment

TABLE 1 Measurement scenarios

| Scenario	f (GHz)	h_r (m)	h_g (m)	d_b (m)	θ (°)	Description
S1	28, 32.4, 38	14	2	8, 12, 16, 20, 24, 30, 40, 50, 60, 70, 80, 90, 100, 110	56, 45, 37, 31, 27, 22, 17, 13, 11, 10, 9, 8, 7, 6	Main scenario for diffraction loss: a TX is 2 m above the ground and a RX is on the rooftop
S2	32.4	14	2	16, 20, 30, 50, 80, 110	37, 31, 22, 13, 9, 6	Scenario to check reciprocity: a TX is on the rooftop and a RX is 2 m above the ground
S3	32.4	14	4	10, 20, 25, 50, 75	45, 27, 22, 11, 8	Scenario to verify diffraction coefficients: a TX is 4 m above the ground and a RX is on the rooftop
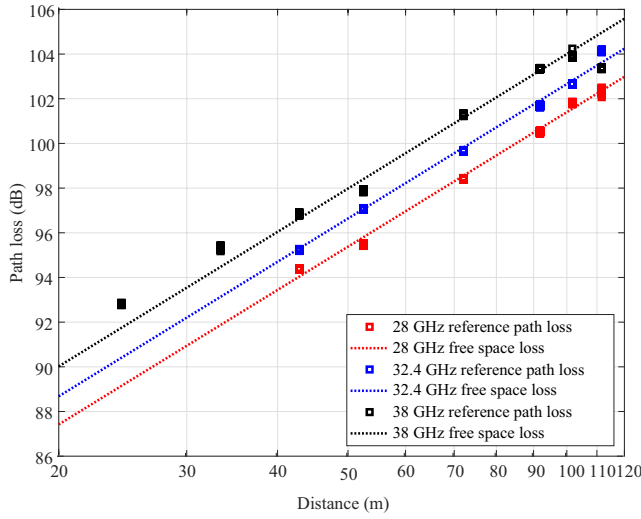
FIGURE 6 Reference path loss measurement results

component. The diffraction loss can be calculated by comparing the excess loss to the free space loss, as represented by

$$L_{DL} = L_{PL} - L_{FSL}(d), \tag{10}$$

where the diffraction loss is denoted by L_{DL}. In Figure 7, the diffraction-loss measurements are represented by circles. As the figure shows, the diffraction loss increases with the distance from the edge to the RX, the diffraction angle, and the frequency. If diffraction losses were successfully extracted from the power-delay profile measurements, then, the diffraction losses should be reciprocal when the TX and RX antennas are exchanged. We exchanged the locations of the TX and the RX to check the reciprocity. Figure 8 shows that the measurement results of scenarios S1 and S2 had similar diffraction-loss levels.

Figure 9 shows the comparison between the KED model and the measurements. The measurements at all frequencies were gathered, and the geometrical parameters were converted into Fresnel-Kirchhoff diffraction parameters. Fresnel-Kirchhoff diffraction parameters can be computed using

$$v = 2\sqrt{\frac{d_1 + d_2 - d}{\lambda}}. \tag{11}$$

When the Fresnel-Kirchhoff diffraction parameter was about 5, the diffraction-loss measurements were approximately equal to the KED model. However, most of the measurements showed larger losses than the KED model when the Fresnel-Kirchhoff diffraction parameter was larger than 10. Consequently, the KED model was not suitable for the environment of Figure 1 because of a high Fresnel-Kirchhoff diffraction parameter is caused by a high frequency, long distance, and large diffraction angle.
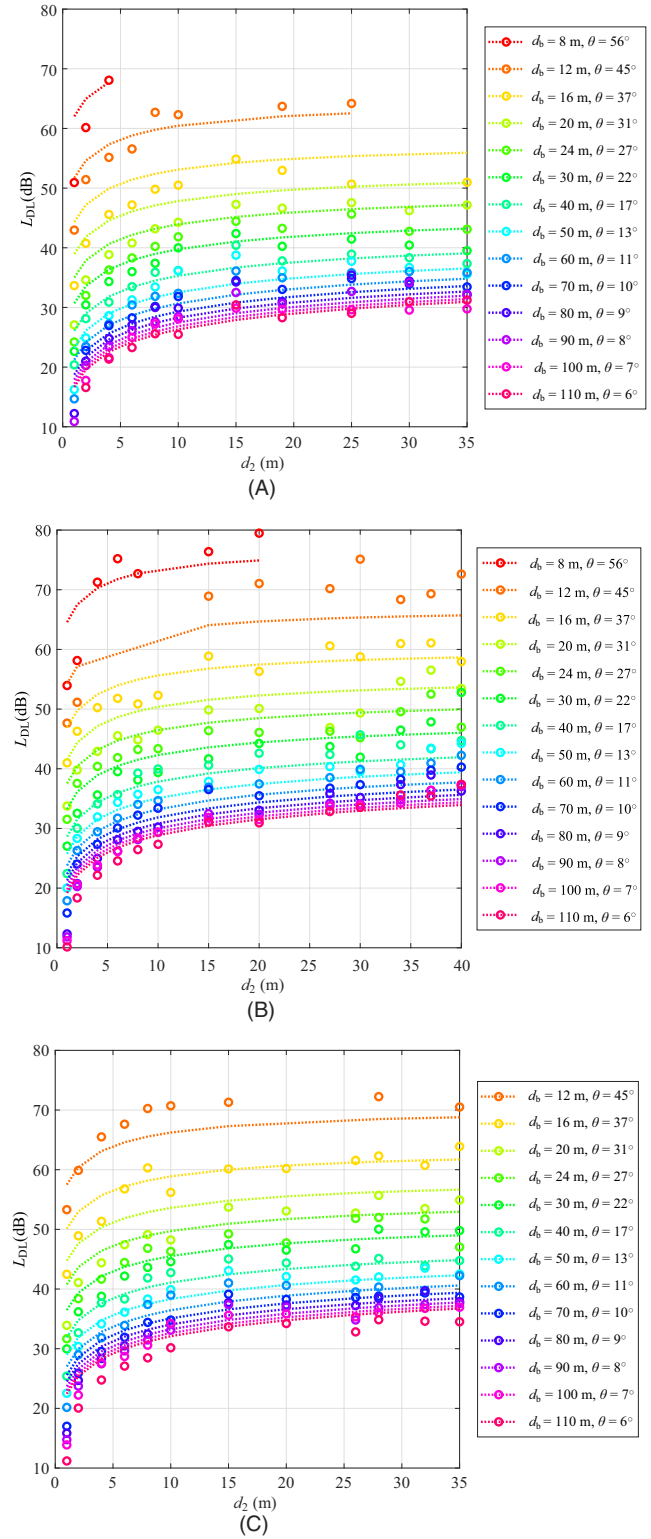

FIGURE 7 Diffraction-loss measurements (circles) and the proposed approximation (dot lines): (A) 28 GHz, (B) 32.4 GHz, and (C) 38 GHz

To compare the GTD model and the measurements, we divided the diffraction loss into a distance-dependent part and a distance-independent part based on (6), which is represented by
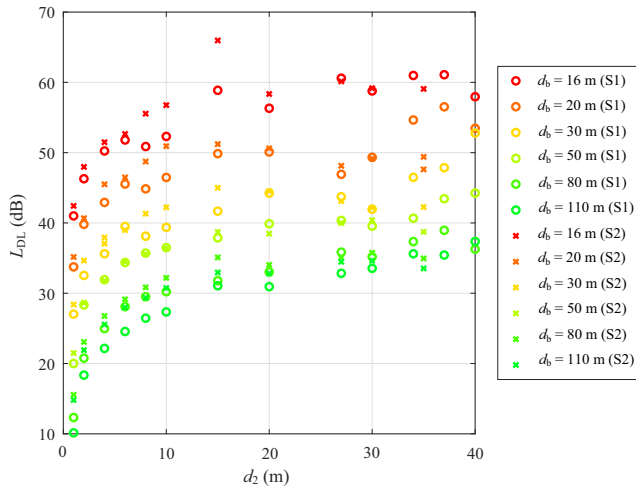
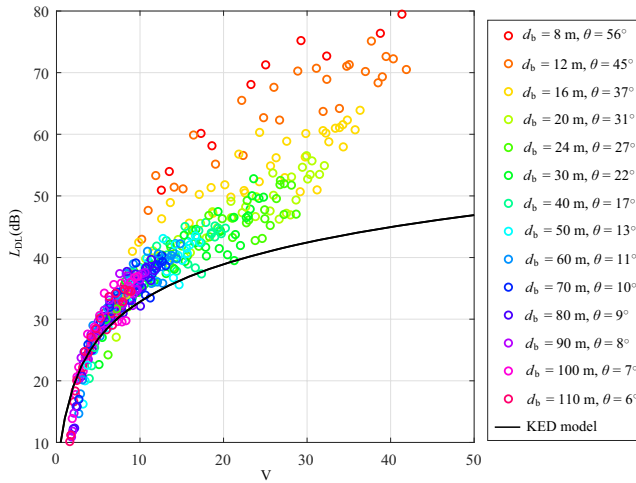**FIGURE 8** Comparison between measurements of scenarios S1 (ground-to-rooftop) and S2 (rooftop-to-ground)

FIGURE 9 Comparison between the KED model (black line) and measurements (circles)

$$L_{\text{DL}} = L_{\text{dist}} + L_{\text{DC}}, \tag{12}$$

where

$$L_{\text{dist}} = 20 \log \left(\frac{\sqrt{d_1 d_2 (d_1 + d_2)}}{d} \right) \tag{13}$$

and

$$L_{\text{DC}} = L_{\text{PL}} - L_{\text{FSL}}(d) - L_{\text{dist}}. \tag{14}$$

A distance-dependent part and a distance-independent part of the diffraction loss are denoted by L_{dist} and L_{DC}, respectively. A distance-independent part is determined by an absolute value of a diffraction coefficient based on the GTD model. Figure 10 shows the distance-independent part of the diffraction losses based on the measurements in scenario S1.
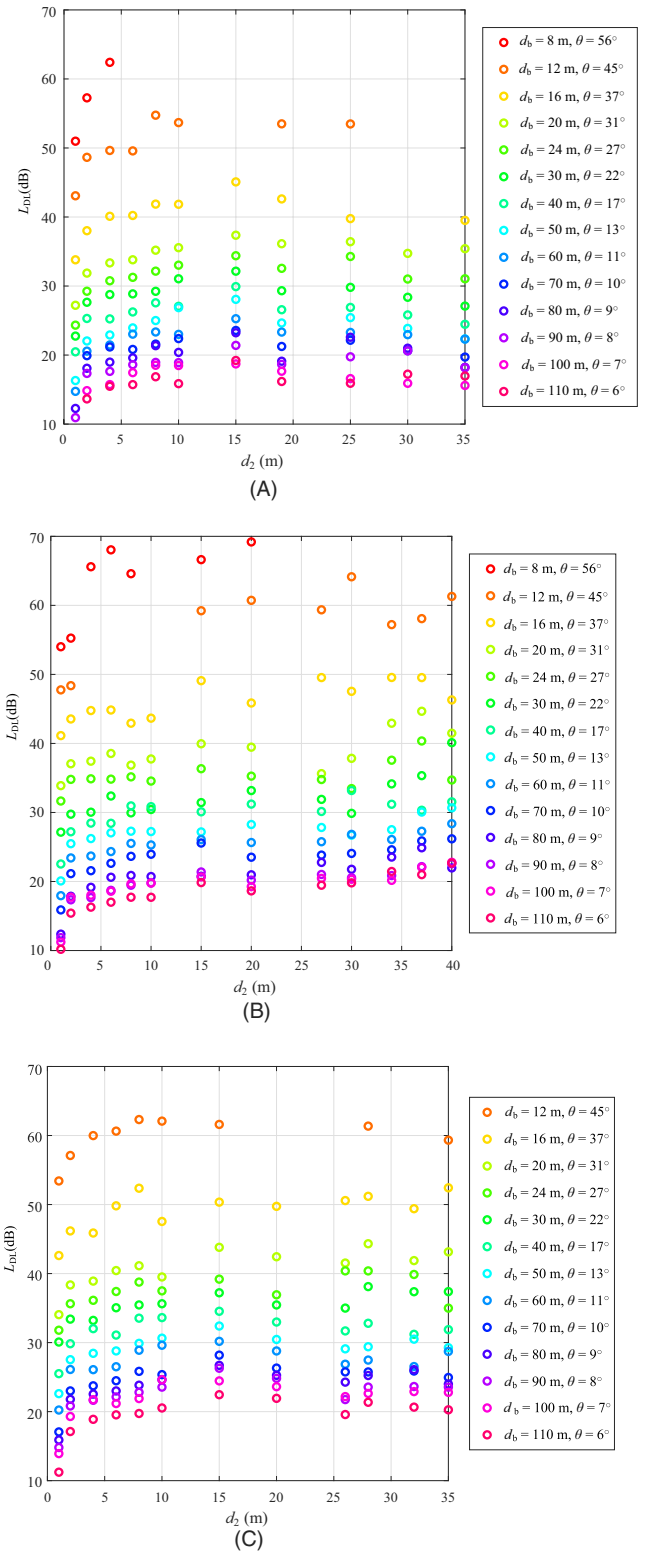

(A)

(B)

(C)

FIGURE 10 Distance-independent part of diffraction-loss measurements: (A) 28 GHz, (B) 32.4 GHz, and (C) 38 GHz

As the figure shows, L_{DC} hardly increases when the distance from the edge to the RX is longer than 2 m. In the far region after 2 m, L_{DC} can be a constant determined by the diffraction angle and the frequency as in the GTD model. To verify that
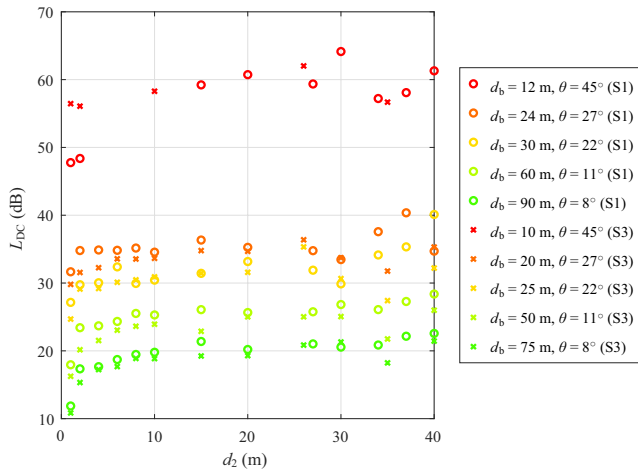
FIGURE 11 Comparison between measurements of the scenarios S1 (2 m) and S3 (4 m)
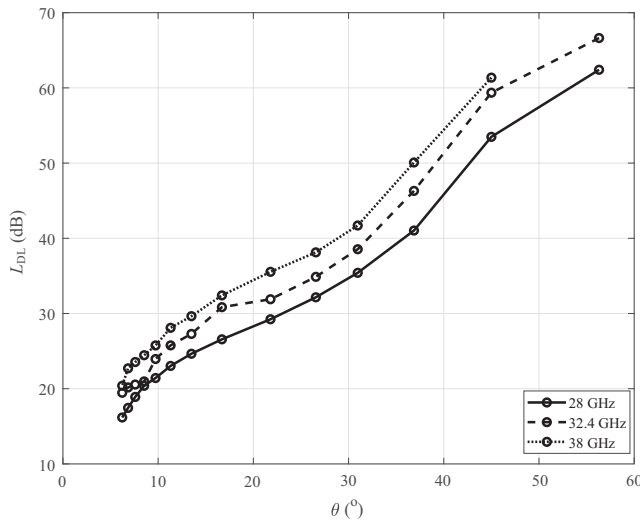

FIGURE 12 Linear relationship between the distance-independent part of the diffraction loss and diffraction angle

L_{DC} does not change with distance, we measured the diffraction losses when the TX locations changed but the diffraction angles were fixed. Figure 11 shows the comparison between the measurements in scenarios S1 and S3, and they showed negligible differences.

Figure 12 shows the median values of L_{DC} after 2 m. They almost linearly increased with the diffraction angles. In this paper, we propose a linear approximation of the L_{DC} as

$$L_{DC} \approx 0.5702 \cdot f + 0.9078 \cdot \theta - 4.9056. \quad (15)$$

The linear relationship between the diffraction angle and diffraction loss was also observed in [17], where the propagation length was fixed to 3 m. For our measurements, the distance-independent part of the diffraction loss was well-fitted to a linear approximation. In this study, the distance-dependent part of the diffraction loss was calculated based on the GTD assumption and the distance-independent part of the diffraction loss was calculated by a linear approximation with a diffraction angle and frequency. We then computed the diffraction loss based on frequency and geometrical parameters using (12), (13), and (15). Figure 8 shows the comparison between the proposed approximation and measurement results, and they are found to match well. The mean error is –0.038 dB and the standard deviation of error is 2.395 dB, where d_2 is longer than 2 m.

5 | CONCLUSION

In this study, we conducted diffraction-loss measurements at 28 GHz, 32.4 GHz, and 38 GHz when a millimeter wave propagates over a building rooftop by diffraction. We also compared the measurement results and theoretical models, such as the KED model and GTD model. The measurement results exhibited higher losses than the KED model, especially with large Fresnel-Kirchhoff diffraction parameters. Large Fresnel-Kirchhoff diffraction parameters are given in environments of high frequencies, long distances, and high diffraction angles. To analyze the relationship between the diffraction losses and distance, the assumption of GTD models was applied. Consequently, regardless of the distance, the diffraction coefficients were shown to be constant in the far regions. Based on the measurements, we proposed a linear approximation of the diffraction loss related to a diffraction coefficient that is determined by the diffraction angle and frequency. The proposed model facilitates diffraction-loss calculation based on geometrical parameters and frequency.

ORCID
Kyung-Won Kim [iD] https://orcid.org/0000-0002-9663-9954
Juyul Lee [iD] https://orcid.org/0000-0002-5851-0615
Young Keun Yoon [iD] https://orcid.org/0000-0002-2062-1432

REFERENCES

1. J. Walfisch and H. L. Bertoni, *A theoretical model of UHF propagation in urban environments*, IEEE Trans. Antennas Propag. **36** (1988), no. 12, 1788–1796.

2. V. Erceg, A. J. Rustako, and R. S. Roman, *Diffraction around corners and its effects on the microcell coverage area in urban and suburban environments at 900 MHz, 2 GHz, and 6 GHz*, IEEE Trans. Veh. Technol. **43** (1994), no. 3, 762–766.

3. J. S. Lu et al., *Site-specific models of the received power for radio communication in urban street canyons*, IEEE Trans. Antennas Propag. **62**(2014), no. 4, 2192–2200.

4. D. Chizhik and J. Ling, *Propagation over clutter: physical stochastic model*, IEEE Trans. Antennas Propag. **56** (2008), no. 4, 1071–1077.

5. H. Fujii et al., *Extension of clutter loss calculation for recommendation ITU-R P.452*, in Proc. Int. Symp. Antenna, Propag. EM Theory (Guangzhou, China), 2010, pp. 477–480.

6. Recommendation ITU-R P.452-16, *Prediction procedure for the evaluation of interference between stations on the surface of the Earth at frequencies above about 0.1 GHz*, 2015.

7. K. Zhao et al., *Channel characteristics and user body effects in an outdoor urban scenario at 15 and 28 GHz*, IEEE Trans. Antennas Propag. **65** (2017), no. 12, 6534–6548.

8. P. Kyosti et al., *Map-based channel model for evaluation of 5G wireless communication systems*, IEEE Trans. Antennas Propag. **65** (2017), no. 12, 6491–6504.

9. J.-H. Lee, J.-S. Choi, and S.-C. Kim, *Cell coverage analysis of 28 GHz millimeter wave in urban microcell environment using 3-D ray tracing*, IEEE Trans. Antennas Propag. **66** (2018), no. 3, 1479–1487.

10. R. J. Luebbers, *Finite conductivity uniform GTD versus knife edge diffraction in prediction of propagation path loss*, IEEE Trans. Antennas Propag. **AP-32** (1984), no. 1, 70–76.

11. H. Mokhtari and P. Lazaridis, *Comparative study of lateral profile knife-edge diffraction and ray tracing technique using GTD in urban environment*, IEEE Trans. Veh. Technol. **48** (1999), no. 1, 255–261.

12. M. Albani et al., *Shielding effect of a thick screen with corrugations*, IEEE Trans. Electromagnetic Compatibility **40** (1988), no. 3, 235–239.

13. D. Erricolo, *Experimental validation of second-order diffraction coefficients for computation of path-loss past buildings*, IEEE Trans. Electromagnetic Compatibility **44** (2002), no. 1, 272–273.

14. T. Negishi et al., *Measurements to validate the UTD triple diffraction coefficient*, IEEE Trans. Antennas Propag. **62** (2014), no. 7, 3723–3730.

15. M. Jacob et al., *Diffraction in mm and sub-mm wave indoor propagation channels*, IEEE Trans. Antennas Propag. **60** (2012), no. 3, 833–844.

16. N. Tervo et al., *Diffraction measurements around a building corner at 10 GHz*, in Proc. Int. Conf. 5G Ubiquitous Connectivity (Akaslompolo, Finland), Nov. 2014, pp. 187–191.

17. T. S. Rappaport et al., *Small-scale, local area, and transitional millimeter wave propagation for 5G communications*, IEEE Trans. Antennas Propag. **65** (2017), no. 12, 6474–6490.

18. J. Lu et al., *Measurement and characterization of various outdppr 60 GHz diffracted and scattered paths*, in Proc. IEEE Military Commun. Conf. (San Diego, CA, USA), Nov. 2013, pp. 1238–1243.

19. H. R. Anderson, *Building corner diffraction measurements and predictions using UTD*, IEEE Trans. Antennas Propag. **46** (1998), no. 2, 292–293.

20. S. Soni and A. Bhattacharya, *Roof-top modeling of building for microcellular systems using double diffraction coefficient*, in Proc. Int. Conf. Comput. Devices Commun. (Kolkata, India), Dec. 2009, pp. 1–4.

21. K.-W. Kim et al., *Diffraction loss model based on 28 GHz over-rooftop propagation measurements,* in Proc. IEEE Veh. Technol. Conf. (Toronto, Canadal), 2017, pp. 1–5.

22. K.-W. Kim et al., *Clutter loss measurement results at millimeter wave frequency bands*, in Proc. Conf. Korean Institute Electromagn. Eng. Sci. (Korea), 2018 (in Korean).

23. J. C. Schelleng, C. R. Burrows, and E. B. Ferrell, *Ultra-short wave propagation*, Proc. Institute Radio Eng. **21** (1933), 427–463.

24. J. B. Keller, *Geometrical theory of diffraction*, J. Opt. Soc. Am. **52** (1962), no. 2, 116–130.

25. R. G. Kouyoumjian and P. H. Pathak, *A uniform geometrical theory of diffraction for an edge in a perfectly conducting surface*, Proc. IEEE **62** (1974), no. 11, 1448–1461.

26. Recommendation ITU-R P.526-14, *Propagation by diffraction*, 2018.

27. H.-K. Kwon, M.-D. Kim, and J. Liang, *Evaluation of multi-path resolution for millimeter wave channel sounding system*, in Proc. Int. Conf. Inf. Commun. Technol. Convergence (Jeju, South Korea), 2015, pp. 1034–1036.

AUTHOR BIOGRAPHIES

Kyung-Won Kim received his BS degree in electrical engineering from Korea University, Seoul, Rep. of Korea, in 2009, and his PhD degree in computer and radio communications engineering from Korea University in 2015, respectively. Since 2015, he has been with Electronics and Telecommunications Research Institute, Daejeon, Rep. of Korea, where he is currently a senior researcher. His current fields of interest include wireless channel measurement, radio signal processing techniques, channel parameter estimation, and wireless channel modeling.

Myung-Don Kim received his BS and MS degrees in electronics engineering from Dong-A University, Busan, Rep. of Korea, in 1993 and 1995, respectively. Since 1995, he has been with the Electronics and Telecommunications Research Institute (ETRI), where he is currently a principal researcher at the Future Mobile Research Laboratory. From 2017 to 2018, he was the Director of the Mobile RF Research Section. He is currently a Project Leader of the Channel Modeling Research Group. His research interests include wireless channel measurements and modeling. Since 2006, he has been involved in many projects for development of wideband MIMO channel sounder, field measurements, and channel modeling. He has contributed to the development of ITU-R recommendations and reports in Study Group 3 (Propagation), including millimeter-wave propagation models. Since 2014, he is the chairperson of the ITU-R WP3K Draft Group 3K-3A, which studies the prediction methods for short-path outdoor propagation in the frequencies from 300 MHz to 100 GHz.
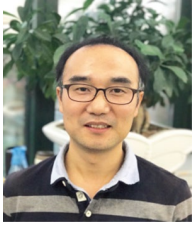
Juyul Lee received his PhD degree in electrical engineering from the University of Minnesota at Twin Cities, USA, in 2010. He was with the Agency for Defense Development, Daejeon, South Korea, from 1998 to 2000. Since 2000, he has been with the Electronics and Telecommunications Research Institute, Daejeon, where he is currently a Principal Researcher with the Telecommunications and Media Research Laboratory. His current research interests include wireless channel modeling, machine learning, and information theory. He has contributed to ITU-R recommendations and reports in Study Group 3 (Propagation) including millimeter-wave propagation models. Since 2017, he has been the Chairman of the ITU-R Correspondence Group 3K-6, which is responsible for studying the impact of higher frequencies (from 6 to 450 GHz) on propagation models and related characteristics.

Jae-Joon Park received the BS and MS degrees in control and instrumentation from Chungang University of Seoul, Rep. of Korea in 1997 and 1999, respectively. He is a principal researcher of Electronics and Telecommunications Research Institute, Daejeon, Rep. of Korea. Since 1999, he has worked on development of smart antennas for FDD/TDD WCDMA system, the WiBro system for broadband wireless internet services, and wideband wireless channel model for next generation mobile communication. His current research interests are channel modeling for millimeter-wave high-speed vehicular wireless communications.

Young Keun Yoon received his BS degree in electrical engineering from Chungbuk National University, Cheongju, Rep. of Korea, in 1991, and his MS and PhD degrees in radio communication engineering from Chungbuk National University, Cheongju, Rep. of Korea, in 1999 and 2007, respectively. Since 2000, he has been working in Electronics and Telecommunications Research Institute, Daejeon, Rep. of Korea, where he is now a senior member. His main research interests are radio propagation, communication, and artificial intelligence based on radio communication.

Young Jun Chong received the BS degree from the Jeju University, Jeju Island, Korea, in 1992, and the MS degree in electronics engineering in 1994 from Sogang University. He also earned a PhD degree in Electronic Engineering from Chungnam National University, Daejeon, Korea, in 2005. Since 1994, he has been working in Electronics and Telecommunications Research Institute, Daejeon, Korea, where he is now a principal researcher. He is currently involved in the research of spectrum engineering. His research interests include RF circuit, systems, and interference analysis. He is a member of KIEES.